Research Article

Journal of Environmental Nanotechnology

Tailoring the Properties of Unsaturated Polyester Composites *via* Graphene Oxide Reinforcement for High-performance Application

M. Karunakaran[1], A. Amutha[1], K. Sharmista Sree[2], Ravi Subban[3*] and C. T. Vijayakumar[4]

[1]Department of Chemistry, Government Arts College, Udumalpet, TN, India
[2]Department of Oral Medicine and Radiology, Yenepoya Dental College, Deralakatte, Ullal, Mangalore, KA, India
[3]Department of Chemistry, Karpagam Academy of Higher Education, Coimbatore, TN, India
[4]Department of Polymer Technology, Kamaraj College of Engineering and Technology (A), S.P.G.C. Nagar, K. Vellakulam, TN, India
Received: 05.07.2025 Accepted: 08.09.2025 Published: 30.09.2025
*subbanravi31@gmail.com

ABSTRACT

This study investigated the synthesis, characterization, and performance of unsaturated polyester resin (UPR) composites reinforced with 1 wt.% graphene oxide (GO). The composites were prepared by mechanically mixing UPR, general-purpose resin (GP), iso marine resin (ISO) and rooflite resin (RL) with GO, followed by ultrasonication and curing. The oxidation of graphene into GO and the generation of resin composites was verified by X-ray diffraction (XRD) and Fourier Transform Infrared spectroscopy investigations. Graphite lacked any noticeable distinctive peaks whereas, characteristic absorption bands at 3350(O-H), 1718 (C=O), 1613 (C=C), 1165 and 1036 cm−1 to C-O-C illustrated the functionalized structure of GO. Characteristic peaks at 2θ=10.27, 30.4 and 2.1 were observed in the XRD spectrum of GO. Scanning electron microscopy revealed improved particle distribution and morphological changes in the resin after GO incorporation. Thermogravimetric analysis and differential scanning calorimetry (DSC) demonstrated increased thermal stability, while the mechanical tests showed improvements in hardness. The DSC curves of the GO sample exhibited a clear exothermic peak at 201°C, and highest tg value of 85.3°C was found in 1% GO composite of ISO resin and in DTG it showed a T_{max} value of 386°C. Tensile, flexural, and compressive strengths of the GO composites are measured and reported. The dielectric strength of the composites also varies based on resin type, with GO improving insulation properties in certain resins. Dielectric value strength value of 5080.0 V/mm for GP resin with 1% GO shows an enhanced overall dielectric performance. A comparison is made among the resin composites of GP, ISO and RL UPR. It was observed that the addition of GO significantly enhanced the thermal, mechanical, and electrical properties of the polyester composites, making them suitable for advanced material applications.

Keywords: Thermoset composites; Unsaturated polyester resin; Graphene oxide composites; TGA and DSC; Mechanical properties; Dielectric strength.

1. INTRODUCTION

Thermosetting plastics play a key role in fostering innovation and researchers have been able to investigate novel applications of them in a variety of industries due to their adaptable qualities. The commercial potential of thermosetting plastics had increased due to its key features, which include low viscosity in the uncured state, configurable modulus, high heat stability, ease of processing, and compatibility with fillers. In spite of that, problems such as poor chemical resistance, low electrical conductivity, and restricted thermal stability should be addressed. Unsaturated polyester resin (UPR) - graphene oxide (GO) composites have gained significant attention due to their improved mechanical, thermal, and electrical properties, making them highly suitable for a variety of industrial applications. The addition of GO to UPR has enhanced the composite's overall performance, increasing its strength, flexibility, and resistance to corrosion (Kim *et al.* 2010).

Graphene oxide is a single layer of graphite oxide with oxygen-containing functional groups like hydroxyl, epoxy, carbonyl, and carboxyl on its basal planes and edges which can alter the Van der Waals forces during the interactions with solvents and polymer matrices. Large amounts of GO can be made from easily accessible, inexpensive natural graphite. Intercalated or exfoliated GO composites are formed when polar molecules or polymers contact strongly with the oxygen groups on GO. Extensive research had been conducted on GO-based polymer composites, making interesting enhancements in their mechanical, thermal, and electrical characteristics (Chen *et al.* 2012).

Sor far, only the mechanical strength of composites made of reinforced UPR with GO concentrations of 0.015 and 0.15% had been measured

and reported (Zarei, 2024). GO modified epoxy resin (EP)/GO composites (An et al., 2024; Reis *et al.* 2023; Wang et al. 2023), acrylic-epoxy-based nanocomposite (Kumar *et al.* 2023), bio-epoxy/GO composites (Farshidfar *et al.* 2023) were widely studied for their enhanced mechanical, tensile strength, hardness, rheological behaviour, durability, hydrophilicity and thermomechanical behaviour properties. To the best of our knowledge, studies on the integration of GO into the UPR matrix are very scarce. In particular, research on GO-UPR composites remains limited, with notable gaps in studies concerning general-purpose (GP), iso marine (ISO) and rooflite (RL) unsaturated polyester resin. This study dealt with these gaps by providing an extensive analysis of the synthesis of GO composites using three different types of UPRs: GP resin, RL resins which are ortho and para resins, respectively, and ISO resin, a meta resin. The research covered an exhaustive evaluation of these composites, focusing on their chemical structure, crystallinity, morphology, thermal stability, hardness, mechanical properties, and dielectric characteristics.

2. EXPERIMENTAL SECTION

2.1 Materials

Pure 98% graphite fine powder was purchased from Loba Chemicals Private Limited; India and it was utilized immediately without further purification. Sulfuric acid was lab-grade, while all other compounds employed in this investigation were analytical grade. Potassium permanganate and sulfuric acid were procured from Emplura® Indian and potassium nitrate from Spectrum Chemicals, India. 35% hydrogen peroxide was purchased from Qualigenes, India. General-purpose resin, ISO resin, RL resin, catalyst, and accelerator were obtained from S.R. Resins and Chemicals Industries, Coimbatore, Tamil Nadu, India.

2.2 Methods

2.2.1 Synthesis of GO

The procedure followed for preparation of graphene oxide was that described by Marcano *et al.* (2010). Hummers' reagents were utilized in this procedure along with extra $KMnO_4$. After adding concentrated H_2SO_4 (69 mL) to a mixture of graphite flakes (3.0 g, 1 wt. equiv.) and $NaNO_3$ (1.5 g, 0.5 wt. equiv.), the mixture was cooled to 0°C using an ice bath to keep the reaction temperature below 20°C. After raising the temperature of mixture to 35°C, it was stirred for seven hours. An additional 9.0 g of $KMnO_4$ (3 wt. equiv.) was then added in a single portion, and the reaction was stirred for 12 hours at 35 °C. Then the reaction mixture was allowed to cool room temperature and then it was transferred onto ice (approximately 400 mL) containing 3 mL of 30% H_2O_2. The remaining solid material was washed with 200 mL of ethanol, 200 mL of 30% HCl, and 200 mL of water. The suspension was then centrifuged for about 10 minutes at 4000 rpm, and the supernatant was discarded each time. To obtain GO powder, the residue from this process was coagulated with 200 mL of ether and the resulting suspension was centrifuged. The residue obtained was throughly washed with large quantities of water. After the washing process is over, the solid residue was dried in an oven at 90°C for 24 hours.

2.2.2 Synthesis of UPR / GO Composites

The appropriate amount of unsaturated polyester resin, 1.5 mL of cobalt naphthenate per 100 g of resin, and 1 weight percent GO were mechanically stirred to fabricate the composites. The final product was then subjected to ultrasonication (Labmann, India). The material was degassed, and the reaction mixture was added with an initiator and the recommended amount of methyl ethyl ketone peroxide (MEKP) (1.5 mL per 100 g of resin). The obtained mixture was then put into glass molds after continuous stirring to prevent the production of air bubbles. The interiors of the glass molds were painted with Mansion wax polish before the material was poured into them. Two different settings were used to cure the produced glass molds. They were first cured for a day at room temperature and then for two hours in a hot air oven set to 80 to 90°C. After this, the glass molds were allowed to cool to ambient temperature and dried. The percentage of GO added to three different unsaturated polyester resins are shown in Table 1.

Table 1. GO (%) present in various samples under study

Sample Code	Resin Used	Wt. % of GO Added
A-1	GP	0
AG-1	GP	1
B-1	ISO	0
BG-1	ISO	1
C-1	RL	0
CG-1	RL	1

2.3 Characterization

2.3.1 Fourier Transform Infrared Spectroscopy (FTIR)

Using an ATR mode Bruker alpha II - FTIR Spectrometer, (Germany) the IR spectra of the graphite used, synthesized GO, all the UPRs used, and their GO composites were recorded from 4000 cm^{-1} to 400 cm^{-1}.

2.3.2 X- ray Diffraction Analysis (XRD)

Using an advanced Bruker D8 Advance diffractometer (Germany) with Cu source with a wavelength of 1.54 nm, X-ray diffraction patterns at 40 kV and 40 mA, scan rate 0.02° s^{-1}, and 2θ = 10° - 70°, the

percentage crystallinity of graphite, GO and composites were analysed by XRD method.

2.3.3 Scanning Electron Microscopic Analysis (SEM)

The SEM images were captured using the TESCAN VEGA3 SBH tungsten thermionic emission SEM system, which had a resolution of 2 nm.

2.3.4 Differential Scanning Calorimetry (DSC)

The primary thermal transitions of the UPRs and their GO composites were determined using Proteus software and differential scanning calorimetry (DSC) in a NETZSCH DSC 350 SIRIUS (Germany) apparatus. The glass transition temperature (T_g) of the virgin UPRs and their GO composites was evaluated from the DSC data. The thermogram was recorded using 7-8 mg of each sample in a very clean nitrogen atmosphere at a scan rate of 10°C/min.

2.3.5 Thermogravimetric Analyses (TGA)

Thermogravimetric Analysis was used to determine the thermal stability of individual UPR and the corresponding GO composites. NETZSCH model NJA – STA 2500 Regulus (Germany) was used to determine the thermal deterioration of GO, three UPR, and their composites. It operates in a nitrogen atmosphere at a scan rate of 10°C/min. A highly clean nitrogen atmosphere was used, and 1 to 2 mg of each sample was used to record the thermogram. For this investigation, the main components used were, an Al_2O_3 crucible, 40 mL of purified gas, and 60 mL of productive gas (for a total of 100 mL).

2.3.6 Mechanical Properties

2.3.6.1 Hardness Analysis

The pure and composite resin plates were tested for hardness using a Rockwell cum Brinell Hardness testing machine by M/s Saroj Engineering Udyog PVT LTD, Jaysingpur, India. The plate samples were subjected to indentation using a suitable ball indentor. The instrument has a maximum capacity of 60 kg force. After the plates were tested for hardness three times, the average of the individual values was used to find the sample's exact hardness value.

2.3.6.2 *Tensile, Flexural and Compressive Strength Analysis*

The Tinius Olsen Model H50 KN UTM (UK) with Horizon software (a servo-controlled machine) was used to measure the tensile, flexural, and compressive strengths of pure resins and their GO composites. The instrument has a maximum load capacity of 50 N. For both the tensile and flexural strength tests, the strain rate was 1 mm/min. The compressive strength strain rate was 0.5 mm/min. The test samples, which were solely utilized for tensile and flexural strengths, had dimensions of 100 mm in length by 25 mm in breadth. An exception was noted in the case of compressive strength, when processed samples were tested using dimensions of 25 mm × 25 mm.

2.3.7 Dielectric Strength Determination

All three UP resins and their GO composites were tested for dielectric strength. In order to evaluate the dielectric strength, SEV Electrical Equipment's Pvt Ltd, located in Mumbai, India, provided the acrylic test cell with electrodes and the AC high voltage tester, which has a range of 0 to 50 kV/50 mA. It was believed to be separated into two sections. 1. Primarily focused on determining the breakdown voltage 2. Determining the dielectric strength was a secondary concern. The breakdown voltage is defined as the specific point at which dielectric resin plates change into conducting resin plates. An alternating current (AC) transformer generates voltages between 0 and 50000, which are measured with a high voltage tester. Volts (V) is the SI unit of voltage. Volts (V) is the SI unit of voltage. The formula

$$\text{Dielectric strength} = \frac{\text{Breakdown voltage}}{\text{Thickness of the plate}} \quad \ldots (1)$$

can be used to get the dielectric strength. Since there was no such thing as an ideal thickness, the actual thickness of the plate cannot be determined by a single value. Thus, the mean of the values, ensured at three distinct spots on the plates, was considered. At last, the precise thickness of the plate was determined. Dielectric strength was measured in V/mm.

3. RESULTS AND DISCUSSION

3.1 FTIR Studies of Pure Resins and Their GO Composites

The FTIR spectra of graphite, GO, pure UPRs and GO-composites of UPRs, are shown in Fig. 1(a and b). Graphite lacks noticeable peaks due to its high degree of purity and inertness (Bera *et al.* 2018).

Ester carbonyl stretching vibration appeared as a prominent peak at 1725 cm^{-1} in the infrared spectra of pure GP resin (Nosal *et al.* 2021). The vibration of the aromatic skeleton is exhibited by a peak at 1592 cm^{-1} whereas the bending vibration of the methyl group is responsible for the band at 1447 cm^{-1} (Rusmirovic *et al.* 2016). The stretching vibration of C-H bond in the methyl group and the methylene group gives rise to an absorption band at 1488 cm^{-1} (Nosal *et al.* 2021). C-O stretching vibration is responsible for the absorbance band at 1254 cm^{-1} (Misra *et al.* 2006), O-C=O group is responsible for the band at 1054 cm^{-1}, and di-substituted ortho benzene ring is responsible for the sharp and intense bands at 746 cm^{-1} and 698 cm^{-1} (Adeosun *et al.* 2015).

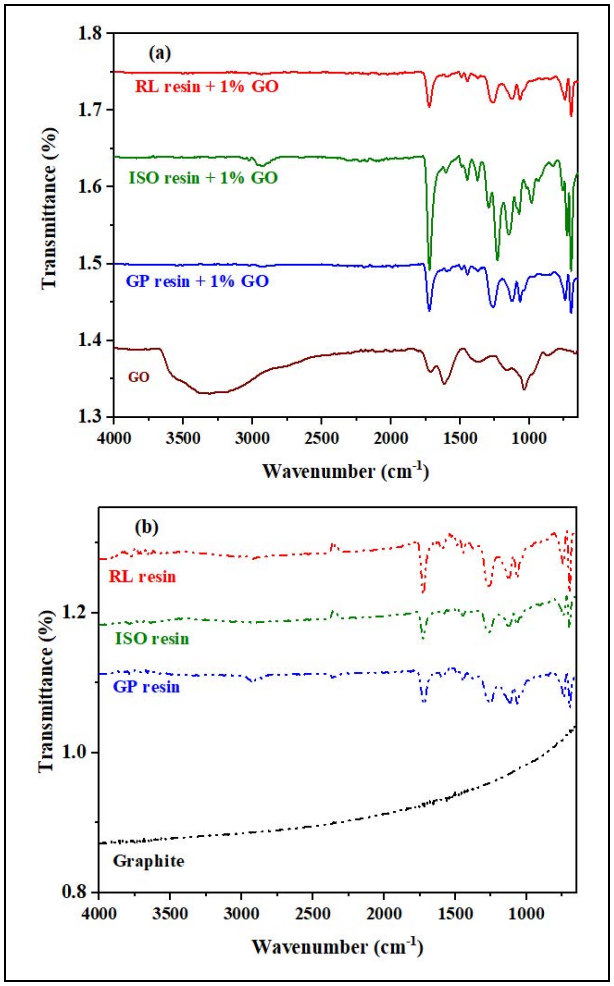


Fig. 1: (a) Infrared spectra of pure GO and UPR-GO composites (b) infrared spectra of graphite and pure UPRs

The broad peak at 3350 cm^{-1} is due to the stretching vibration of hydroxyl group (Hosseini *et al.* 2022). This broad peak indicates that the surface of GO may include hydroxyl groups. The identification of carbonyl (C=O) stretching vibration is responsible for the sharp peak at 1718 cm^{-1}(Sudesh *et al.* 2013). The C=C stretching vibration appeared as a sharp signal at 1613 cm^{-1}. The peak at 1036 cm^{-1} is due to C-O-C stretching (Marcano *et al.* 2010).

The broad peak at about 3400 cm^{-1} is typically absent in the infrared spectra of GO when GO composites with unsaturated resin are taken into consideration. The absence of this indicates that the hydroxyl groups may be considerably decreased during composite formation due to interactions between the polymer matrix and the functional groups of GO. It also suggests that the incorporation of GO into the polymer matrix promotes a smoother transition of molecular characteristics and influences the overall thermal and mechanical properties of the yielded composite material (Liu *et al.* 2016). The other absorption bands are due to native resin molecules.

3.2 X-ray Diffraction Studies

Fig. 2(a) and 2(b) display characteristic peaks at 2θ in the XRD of graphite and GO, respectively between 10° to 70°. The XRD spectrum of graphite (Fig. 2(a)) showed two main peaks at 2θ = 26.46° and at 2θ = 54.62° that closely matched with the standard graphite values reported in JCPDS file 012-0212. This uniformity was attested to the high crystalline quality and purity of the graphite powder used in the investigation. The XRD spectrum of GO is shown in Fig. 2(b). The crystalline nature and phase structure of the obtained materials were ascertained with the help of XRD analysis. The GO diffractogram showed a noticeable peak at 2θ=10.27 that matched the (001) plane and indicated an interlayer spacing of 0.86 nm (Aghehrochaboki *et al.* 2019). This diffractogram displayed a Bragg peak approximately at 2θ = 30.4, as well as a strong crystalline peak at 2θ = 42.1° with d spacing of 0.21 nm, which was consistent with JCPDS Card No. 22–1086 and corresponds to the (100) plane (Celebi *et al.* 2017).

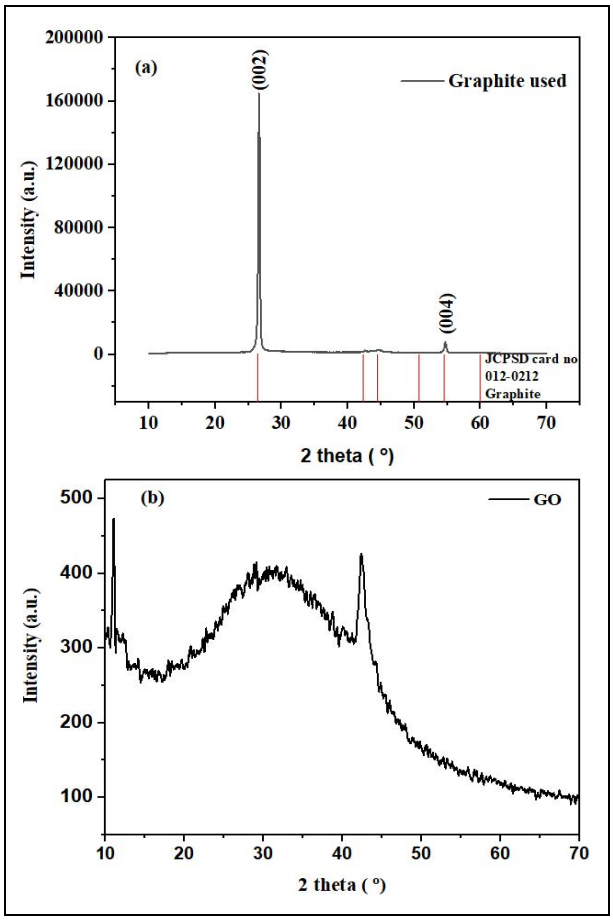


Fig. 2: (a) XRD of graphite and (b) XRD of graphene oxide

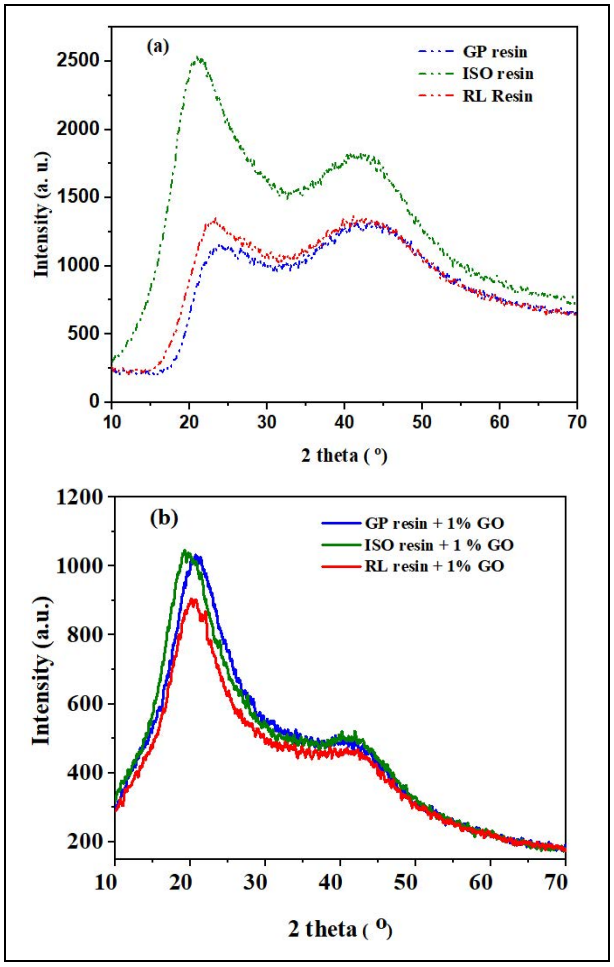


Fig. 3: (a) XRD of pure resins and (b) XRD of GO composites of resins

The XRD of pure resins used in this investigation at 2θ between 0° and 70°are shown in Fig. 3(a). The XRD spectra of all three unsaturated polyester resins exhibited similar patterns, consisting of two wide peaks, one at 2θ = 16.75° with a d-spacing of 0.53 nm, and another at 2θ = 41.91° with a d-spacing of 0.33 nm. Similarly, the diffractogram of pure ISO resin (B-1) showed two prominent peaks: one at 2θ = 21.26° with a d-spacing of 0.42 nm, and another at approximately 2θ = 41.75° with a d-spacing of 0.22 nm. Additionally, the diffractogram of another sample of pure RL resin (C-1) showed a broad peak around 2θ = 22.14° with a d-spacing of 4.0118 nm, and another broad peak at 2θ = 43.23° with a d-spacing of 2.0911 nm. The intermolecular interaction in the long polymer chain structure, the relatively high number of crystal defects, and the amorphous structure of the UPR (Ambika *et al.* 2017) were the causes of this peak broadening.

The XRD of GO composites of resin is shown in Fig. 3(b). When examining the X-ray diffraction pattern of UPR with 1 wt. % GO composite, an important observation was the diminished intensity or even disappearance of the characteristic reflection peak of GO. This phenomenon is commonly attributed to the exfoliation of the GO sheets and their homogeneous dispersion throughout the polyester matrix (Bora *et al.* 2013). This behaviour was consistent with other GO-based polymer composites, where similar peak reduction or disappearance was observed. For instance, GO dispersed in epoxy, polystyrene, or other polymer matrices showed the same trend in XRD analysis. This suggested a successful exfoliation and intercalation process where GO layers were distributed evenly within the polymer network. The disruption of crystalline structure of GO through dispersion ensured better mechanical, thermal, and electrical properties in the composite, where the polymer matrix interacts effectively with the exfoliated GO sheets (Yang *et al.* 2011). The diffractogram of GP resin GO composites (AG-1) showed two broad peaks: one at 2θ = 20.37° with a d-spacing of 0.44 nm, and another at 2θ = 41.62° with a d-spacing of 0.22 nm. Similarly, the diffractogram of pure RL resin GO composites (BG-1) revealed two prominent peaks: one at 2θ = 19.02° with a d-spacing of 0.47 nm, and another at approximately 2θ = 42.04° with a d-spacing of 0.21 nm. Additionally, the diffractogram of another sample of pure RL resin GO composites (CG-1) showed a broad peak around 2θ = 22.38° with a d-spacing of 0.39 nm, and another broad peak at 2θ = 41.71° with a d-spacing of 0.21 nm.

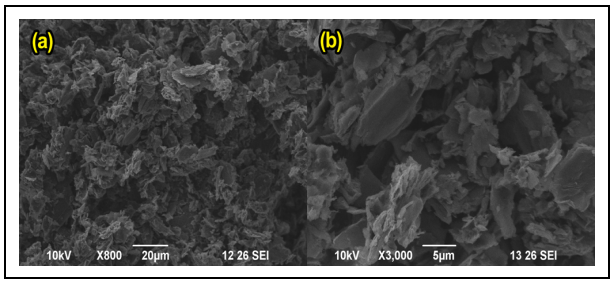


Fig. 4: (a) Low (G-1) and (b) high (G-2) magnified SEM images of graphite

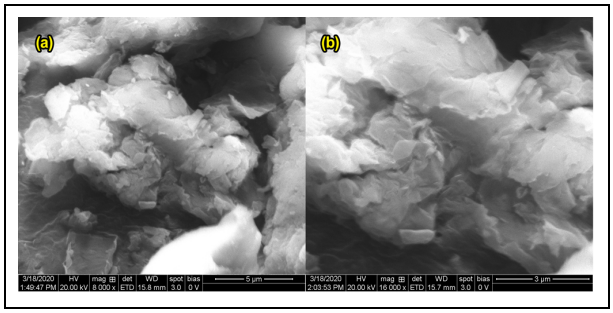


Fig. 5: (a) Low (GO-1) and (b) high magnified SEM images of graphene oxide (GO-2)

3.3 SEM Analysis

The SEM images of pure graphite (G-1 and G-2) are shown in Fig. 4(a) and (b), where the particles appear to be asymmetrical and flaky. Alshammari *et al.*

(2019) also made similar observations of particles with a mean diameter ranging from 4 to 10 µm. When used as a filler in polymer composites, this flaky morphology plays an important role in deciding the reinforcing qualities and dispersion behavior of graphite.

The SEM images of GO (Fig. 5(a) and (b)) revealed a few stacked sheets with distinct edge defects, similar to that found by Dhali *et al.* (2020). Their thickness is larger than that of a single-layer graphene, likely ranging between 1 - 2 µm, attributed mainly to the presence of oxygen-containing functional groups (Anegbe *et al.* 2024). Fig. 6(a) to 6(f) display SEM images of pure resin and its GO components. The addition of GO to the pristine resin disrupted its smooth texture, resulting in the formation of layered bundles of GO. Notably, in Fig. 6b, 6d, and 6f, a more uniform dispersion of small GO sheets was observed within the polyester matrix, suggesting successful incorporation and distribution of GO throughout the resin (Bastiurea *et al.* 2015b).

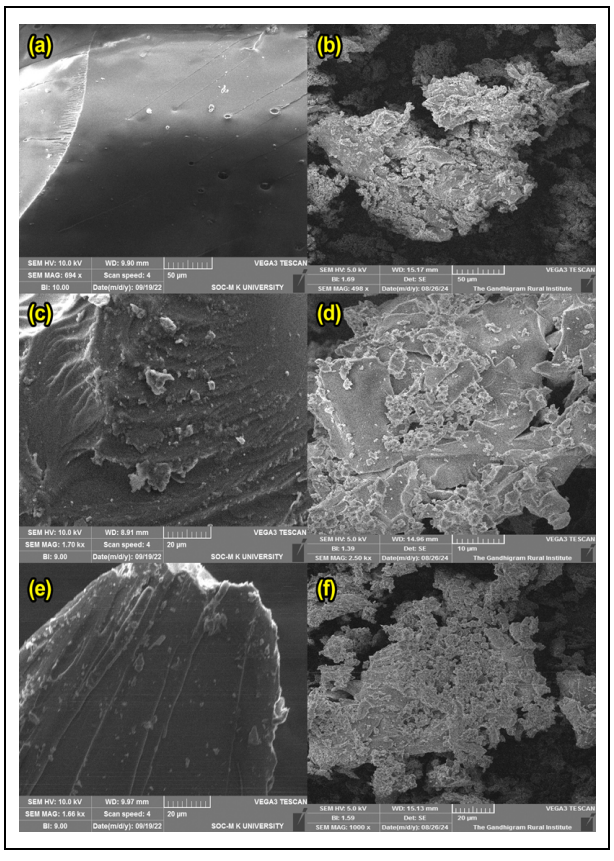


Fig. 6: (a) SEM images of GP resin (A-1), (b) GP resin GO composites (AG-1), (c) ISO resin (B-1), (d) ISO resin GO composites (BG-1), (e) RL resin (C-1), and (f) RL resin GO composites (CG-1)

This improved particle distribution contributed to a more homogeneous surface on the resin, indicating enhanced interaction between GO and the organic matrix. The SEM images also revealed that GO appeared as a thick material with multiple layers, with the spaces between these layers clearly visible. This thickness was attributed to the presence of oxygen-containing functional groups attached to the GO planes, which were responsible for the layered structure(Rochman *et al.* 2019). The observed morphology suggested that during the oxidation process, graphite was effectively exfoliated, leading to the formation of these distinct GO layers.

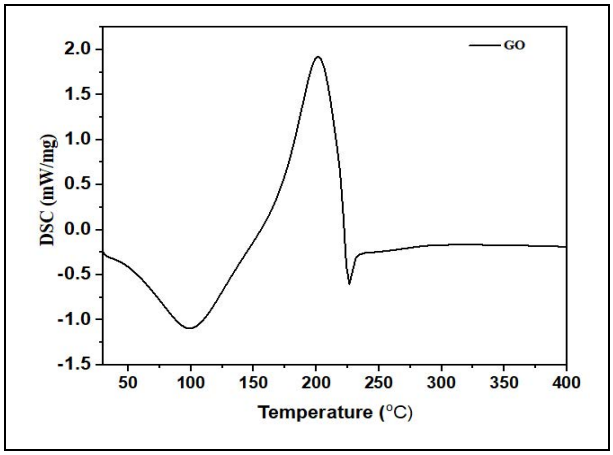


Fig. 7: DSC thermogram of GO

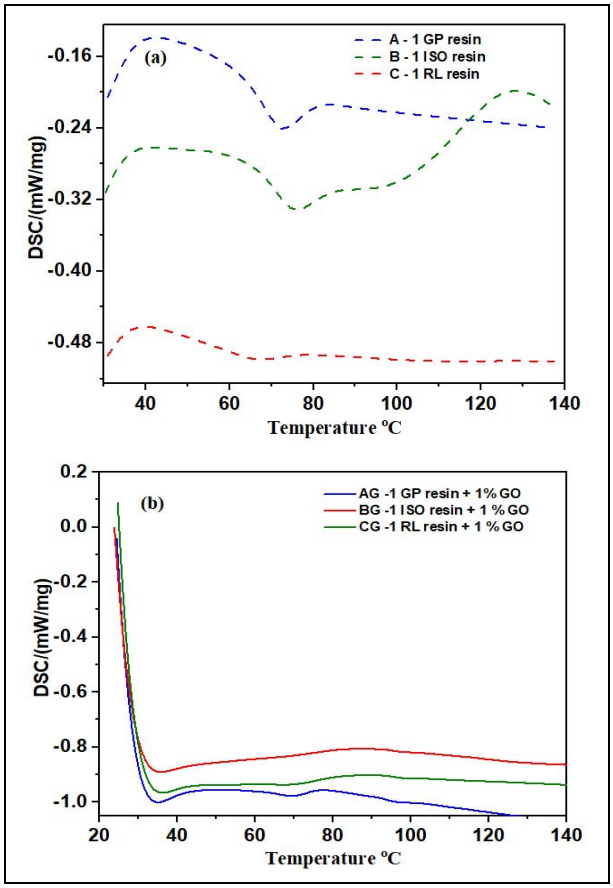


Fig. 8: (a) DSC thermogram of pure resins and (b) DSC thermogram of resin composites

3.4 Differential Scanning Calorimetry (DSC)

The DSC analysis was performed on URPs and its 1% GO composites in an environment containing nitrogen. Fig. 7 displays the DSC thermogram of synthesized GO, while Fig. 8(a) and 8(b) display the thermograms of pure UPRs and their GO composites, respectively. The DSC curves of the GO exhibited a clear exothermic peak at 201°C in Fig. 7, which was consistent with earlier findings (Fryczkowski *et al.* 2013).

It is evident from Fig. 8 that every curve is essentially the same. Due to the common phase transitions, every curve has both an endothermic and an exothermic peak (Bing *et al.* 2021). The enthalpy of the cross-linking reaction at low temperatures with faster cure rates and less time, is responsible for the exothermic peak (Goudarzi *et al.* 2016).

Table 2. DSC results for pure resins and their 1 wt. % GO composites

Sample Code	GO Wt. %	Tg (°C)	ΔCp J/(g°C)
A	0	68.4	0.170
AG1	1	73.9	0.244
B	0	72.4	0.119
BG	1	85.3	0.219
C	0	65.9	0.097
CG1	1	75.3	0.215

The glass transition temperature (T_g) and specific heat capacity (C_p) calculated with the Proteus program are shown in Table 2. The T_g of UPR matrix, GP matrix, ISO resin matrix and RL matrix were determined with and without the addition of GO filler (Bastiurea *et al.* 2015a). The highest T_g value was found for 1% GO composite of ISO resin, followed by 1% GO composite of RL resin and 1% GO composite of GP resin. Since their glass transition temperature is higher than 70.0°C, these composites could withstand modest thermal loads without deforming which is an essential characteristic required for a material to be utilised in electronic gadgets because they could heat up while in use.

The interaction between the filler particles and the polymer matrix raises the T_g values of the UPR matric when GO is added. When the GO particles interact with the polymer chains in a polymer composite, an interfacial zone is formed where the movement of the polymers is considerably decreased. In effect, this interfacial interaction "locks" the polymer chains in place, limiting their mobility. As a result, when GO is introduced to the resin matrix, the GO particles in the cross-linked matrix of the UP resin provides resistance, which significantly reduces the resin's long-chain mobility and the T_g increases. Since the highest T_g value was found for 1% GO composite of ISO resin the interaction between GO and ISO resin could be more when compared to the other two resins. The same trend was observed with respect to specific heat capacity of the polymer matrix and the GO content gives the composite capacity to absorb more heat and makes the polymer more insulative.

3.5 Thermogravimetric Analysis

The analysis by thermogravimetry was done in an environment of nitrogen. Fig. 9(a) shows the outcomes for GO, pure resins, and its GO composites.

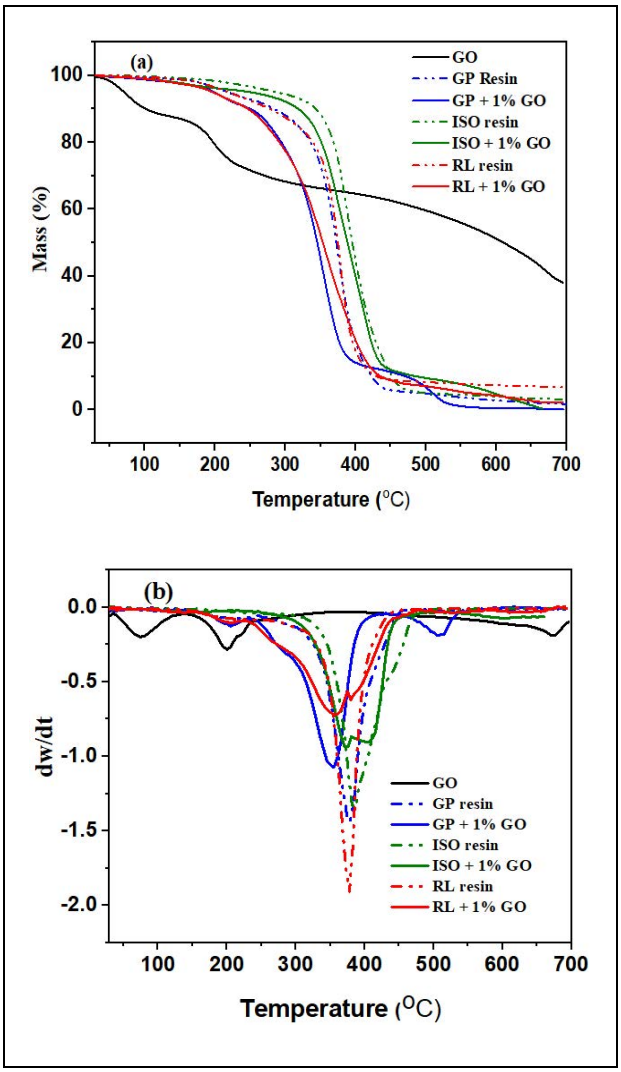


Fig. 9: (a) TGA curve of GO composites and pure resins and (b) DTG curve of GO composites and pure resins

Table 3. Thermogravimetric analysis results for pure resins and their 1 wt. % GO composites

Sample Code	Graphite Wt. %	Temperature Range (°C)						% of char at 650°C	LOI = 17.5 + 0.4 (CY)
		$T_{initial}$	Mass Loss (%)	T_{max}	Mass Loss (%)	T_{final}	Mass Loss (%)		
A-1	0	244	6.8	374	52.4	444	93.9	6.70	20.18
AG1	1	237	8.7	355	66.4	425	87.5	0.35	17.64
B-1	0	305	5.9	386	38.9	487	94.7	3.08	18.73
BG-1	1	280	6.4	375	38.5	455	88.44	1.27	18.00
C-1	0	309	13.8	382	65.6	456	91.3	6.70	20.18
CG-1	1	230	4.4	355	13.6	447	88.1	2.66	18.56

The thermal stability and the effects of varying degrees of oxygen functionalization in the synthesized GO samples were established with the aid of thermogram of GO shown in Fig. 9(a). Due to the GO sample's increased hydrophobicity, the thermogram revealed that the mass loss up to 170 °C is most likely caused by the evaporation of absorbed water (Palomba *et al.* 2021). Above 170 °C to 240 °C, another drop in mass was noticed due to the release of labile oxygen functional groups, such as carboxylates, are eliminated, and CO_2 from the GO sheets (Edwards *et al.* 2022). As the temperature rises over 240 °C, the mass loss becomes less pronounced and is associated with the progressive elimination of more stable oxygen functions (Ossonon and Bélanger, 2017) .

The DTG graph typically showed a single-stage decomposition for all the three UPR materials studied. However, for both the GO and the GO composites formed with the resins, the DTG graph revealed a two-stage decomposition process. From the TG-DTG curves, various key combustion characteristics could be derived, including $T_{initial}$ which is the temperature at which the actual decomposition of the material begins; T_{max} the temperature at which the maximum decomposition will occurs, corresponding to the peak in the DTG curve; and T_{final} which marks the temperature at which rapid decomposition ceases, indicating the end of the primary decomposition phase. These three critical temperatures $T_{initial}$, T_{max}, and T_{final} were determined from the derivative thermograms of GO, the pure resin, and their respective GO composites. For pure resins, all three of the critical temperatures were greater than for their 1% GO composites. It can be inferred that the surface of GO has functional groups that contain oxygen, such as carboxyl, epoxy, and hydroxyl. Due to their thermal lability, these groups break down at comparatively lower temperatures, producing gases including water (H_2O) and carbon dioxide (CO_2). In comparison to the neat resin, the breakdown of these functional groups may result in weak spots in the composite and lower its overall thermal stability (Tang *et al.* 2014). The primary cause of the GO composites' lower limiting oxygen index (LOI) value as compared to pure resin is the thermal breakdown of GO, which releases flammable gases, compromises the integrity of the char layer, and may catalyse the combustion process. A decreased LOI results from these conditions, which also impairs the composite's fire resistance (Liu *et al.* 2021).

3.6 Hardness Analysis of UPR and their GO Composites

The results of the hardness test of pure UPRs and their GO composites, performed using a Rockwell and Brinell machine are displayed in Fig. 10 and Table 4. Based on the data, it could be concluded that adding GO to pure UPR makes it harder (Dhanunjayarao *et al.* 2022). The composite AG-1, with 1% GO, showed a 9.91% increase in hardness compared to plain GP resin. Similarly, the composite BG-1, containing 1% GO, experienced an 8.93% rise in hardness relative to plain ISO resin. The composite CG-1, also with 1% GO, exhibited a substantial 28.24% increase in hardness when compared to normal RL resin. The presence of GO particles distributed the applied stress more effectively across the material, thereby reducing the likelihood of plastic deformation. As a result, the composite material exhibited increased hardness and improved resistance to external forces. This enhancement is particularly valuable in applications where durability is essential (Ali *et al.* 2019).

Table 4. Hardness determination analysis results for pure resins and its 1 wt. % GO composites

Sample Code	Wt % of GO	Trial 1	Trial 2	Trial 3	Average Unit (L)
A1	0	49.8	50.3	50.1	50.07
AG1	1	55.1	55.0	55.0	55.03
B1	0	65.9	66.8	66.5	66.40
BG1	1	72.3	72.4	72.3	72.33
C1	0	43.1	43.6	43.2	43.30
CG1	1	55.7	55.3	55.6	55.53

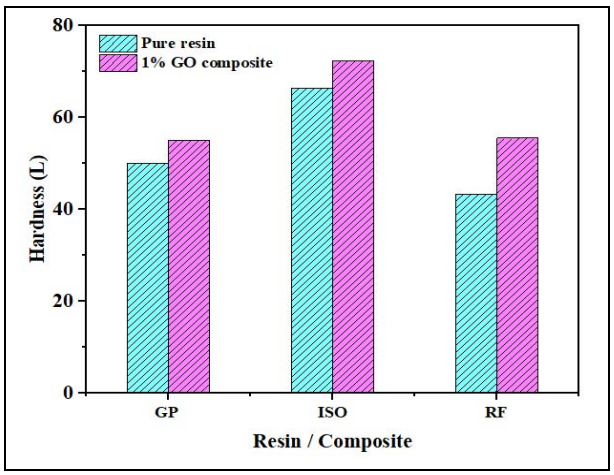


Fig. 10: Hardness analysis results – pure resins and their GO composites

One possible explanation for the increase in hardness properties of GO composites was the large surface area of the GO particles. The extensive surface area of GO allowed for better interaction and bonding with the resin matrix. This increased interaction generated a stronger interfacial adhesion between the GO particles and the matrix, leading to improved load transfer capabilities (Goyal *et al.* 2011). The large surface area also meant that more GO particles could be dispersed throughout the resin, filling more interstices and generating a denser, more uniform composite structure. Additionally, the nano scale dimensions of GO contributed to its ability to reinforce the matrix. The thin, planar structure of GO sheets could effectively bridge micro-cracks and prevent their propagation, enhancing the material's resistance to fracture and deformation (Zhao *et al.* 2020).

The ISO resin composites behaved better than epoxy composites enhanced with fibres or nanoparticles. Strong reinforcing and good compatibility between GO and the RL resin matrix could be the cause of this.

3.7 Mechanical Properties

Consequently, the virgin resin's tensile, flexural, and compressive strengths and GO composites were ascertained. Using the Tinius Olsen - Model H50KL, the composite resin plates were evaluated for tensile, flexural and compressive strengths.

3.7.1 Tensile Analysis

Tensile strength was computed using Horizon software and the Tinius Olsen Model H50 KL instrument. Tensile tests were performed on all of the produced GO composites as well as the pure polymers. The results of the tensile analysis are shown in Fig. 11(a) and Table 5. The stress-strain curves created to gauge the tensile strength of pure resins toughened with GO are displayed in Fig. 11(b). The curve generated for the pure resin and its GO compound showed random arbitrary indiscriminate deformation behavior. The experimental results suggested that all samples, regardless of whether GO filler used, exhibited brittle behavior. This means that the materials fractured without significant deformation when subjected to stress.

Although the strain at which each sample demonstrated brittle behavior varied, the pure RL resin consistently showed the lowest strain at 10.5%. This suggested that the RL resin reached its breaking point with less elongation compared to the other samples, marking the onset of brittle failure. Furthermore, the findings revealed that GO reinforced composites exhibit a bilinear response. Due to this property, the stress-strain curve for these composites has two separate linear areas, corresponding to differing mechanical characteristics prior to and following a specific point of deformation. This bilinear characteristic emphasizes how the type of filler has a major impact on the mechanical properties of the composite. The incorporation of GO alters the stress distribution and failure mechanisms within the composite, leading to a unique response under load.

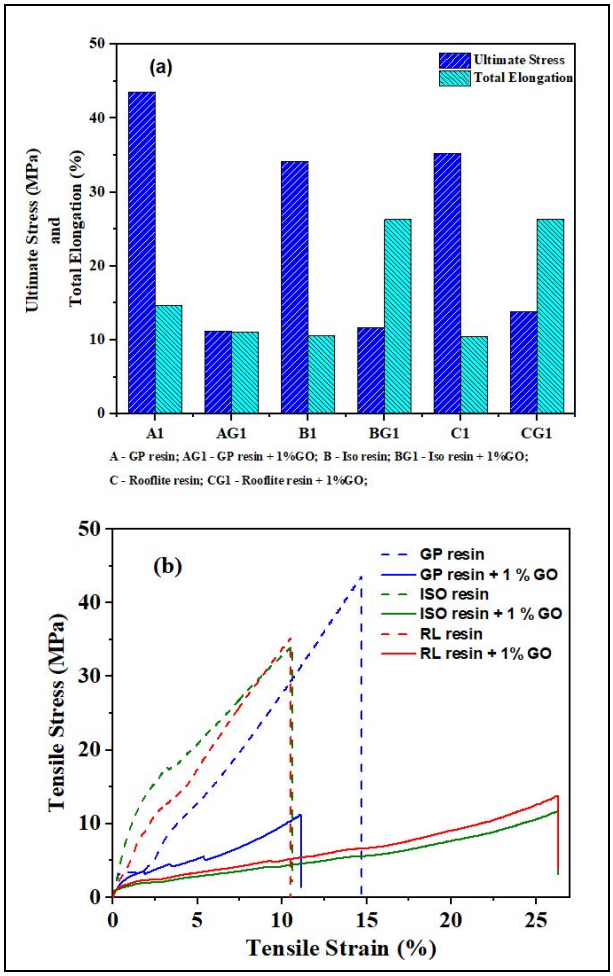


Fig. 11: (a) Tensile strength analysis results for pure resins and their 1 wt. % GO composites and (b) Stress Vs Strain graph for pure resins and their GO composites

The tensile strength of all composites was found to be lower than that of pure resins, as revealed in the current investigation (Suherman *et al.* 2022). The findings indicated a significant reduction in tensile strength for GO composites made with different resins. Specifically, the GO composite made with GP resin experienced a 74.3% loss in tensile strength. Similarly, the GO composite made with ISO resin showed a 65.8% decrease in tensile strength. Also, the tensile strength of the GO composite made with RL resin decreased by 60.7%. The interaction between the GO filler and the resin matrix might cause a drop in the tensile strength of GO composites with different resins. The observed low tensile strength with the GO filler content was explained by the presence of voids or pores, inadequate interfacial adhesion, and particle-to-particle contact (Mourad *et al.* 2020; Jdayil *et al.* 2016). The presence of these stress concentrators disrupts the uniform stress distribution, reducing the composite's ability to withstand tensile forces effectively (Salmah *et al.* 2013).

A recent research proposed that the observed sharp decline in tensile strength in composites incorporating GO filler could be attributed to the formation of an interfacial link between the GO filler and the pure resin matrix. This interfacial bonding changes the overall structural dynamics of the composite material. The GO filler, due to its inherent rigidity, may restrict the mobility of the polymer chains within the resin matrix. This restriction makes difficult the ability of the polymer chains to move and reorient themselves under stress, which is a critical mechanism for absorbing and dissipating mechanical energy. As a result, when an external load is applied, the composite material is more likely to fracture rather than effectively dissipate the mechanical energy, leading to a reduction in tensile strength (Salmah *et al.* 2013).

Table 5. Tensile analysis results for pure resins and its 1 wt. % GO composites

Sample Code	Wt % of GO	Ultimate Force (N)	Ultimate Stress (MPa)	Total Elongation (%)
A1	0	2700	43.6	14.7
AG1	1	1300	11.2	27.1
B1	0	1770	34.2	10.6
BG1	1	1350	11.7	26.3
C1	0	1700	35.2	10.5
CG1	1	1350	13.8	26.3

The mechanical properties of polyester/glass composites were negatively impacted by the addition of fillers including fly ash, alumina, and silica, as noted by Patnaik *et al.* (2009). Similarly, when more than 0.5% of multi-walled carbon nanotubes (MWCNT) were introduced to the epoxy matrix, Mourad *et al.* (2016) found a decrease in the mechanical performance of Kevlar/epoxy composites due to agglomeration. Similar results were also observed in SiC-reinforced aluminum matrix composites (Idrisi and Mourad, 2017).

The impact of GO filler on the polyester composites' elongation at break is presented in Fig. 11 (b). The elastic properties of the resin and its composites were demonstrated by the tensile analysis results of the pure resin and its GO composites. The material's elastic nature could be inferred from the elongation at break. The percentage elongation of the material was reduced compared to that of GO composite of GP resin because it became more brittle. The reduction in elongation at break was mostly caused by the filler stiffening the polymer matrix (Karunakaran *et al.* 2024). In contrast, the amount of disagreement increased when taking into account GO composites made of RL and ISO resin. In light of these two scenarios, the percentage elongation at break values demonstrated the opposite tendency when compared to the composites' tensile strength data (Arora and Gupta, 2023). The significant rise in the % elongation at break values could be attributed to the use of GO as filler, which might act as plasticizers in the polymer matrix. Enhanced load transfer occurred when GO particles were evenly distributed throughout the polymer matrix. This could transfer load efficiently, allowing the tensile qualities of the material to be better utilized. Before breaking, this enhanced interaction might lead to greater ductility and elongation. Graphene oxide particles have the ability to prevent the spread of cracks. A crack might be deflected or bridged when it comes into contact with a GO particle, in which case it needs more energy and elongation to continue spreading.

3.7.2 Flexural Analysis

The Tinius Olsen Model H50 KL with Horizon software was used to calculate flexural strength using the 3-point bend test as per ISO 178. At room temperature, each flexural test was conducted at a set strain rate of one millimeter per minute. Fig. 12 (a) shows flexural analysis results for pure resins and their 1 wt % GO composites. The stress-strain curve for pure resin and its 1 wt % GO composites are shown in Fig. 12 (b). The strain vs stress response was comparable in all pure resins. In the first loading stage, there was some nonlinearity prior to fracture, but the load and deflection vary in a linear relationship. When GO was introduced, the nonlinear functionality disappeared, showing that the composite's flexural strength and strain decreased by the addition of filler (Mourad *et al.* 2020). The flexural strength and elongation at break decreased to 55.4% and 61.7%, respectively, for GP resin and its 1% weight percentage GO composite. The flexural strength reduced by at least 3.8% and the elongation at break dropped by 72.9% for ISO resin and its 1% weight percentage GO composite. In comparison to GP resin and its GO composite, the ISO resin and its composite showed a minimum reduction in flexural strength and a minimal total elongation at breakage.

The flexural strength and elongation at break of GO composites made with RL resin and its 1% weight percentage were 67.9% and 90.6%, respectively. The GO composite made with RL resin exhibited the greatest drop in value in terms of both total elongations at break and flexural strength when compared to the other two resins and their composites. Willis and Masters (2003) reported that adding fillers to a polyester resin matrix decreased the ultimate flexural strength. The increased hardness of the filler material might be the cause of this drop (Nugraha *et al.* 2024).

Table 6. Flexural analysis results for pure resins and their 1 wt. % GO composites

Sample Code	Wt % of GO	Ultimate Force (N)	Ultimate Stress (MPa)	Total Elongation (%)
A1	0	268	86.7	3.90
AG1	1	258	39.5	1.49
B1	0	233	83.8	6.31
BG1	1	578	80.6	1.71
C1	0	222	78.7	5.83
CG1	1	122	25.2	0.544

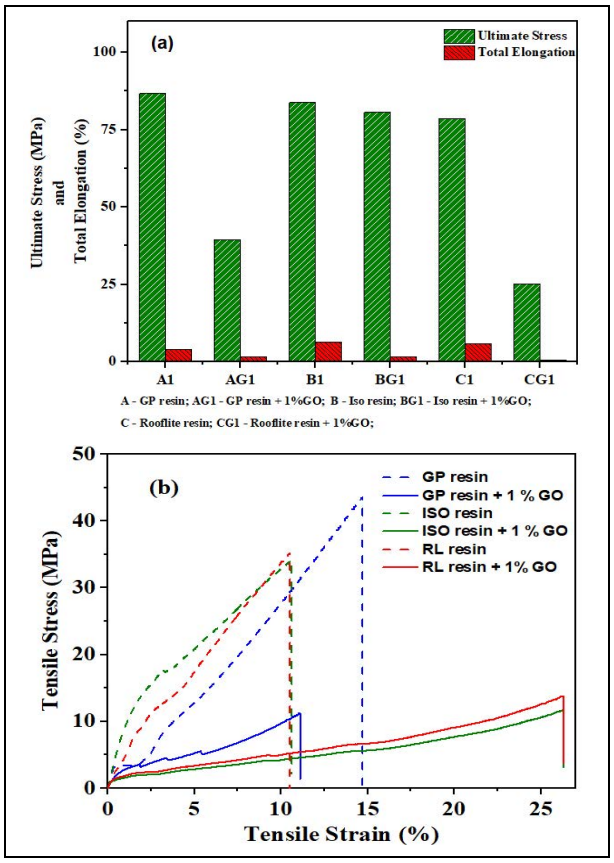


Fig. 12: (a) Flexural analysis results for pure resins and their 1 wt. % GO composites and (b) strain vs stress of pure resins and their 1 wt. % GO composites

This drop is further explained by the filler's inability to withstand pressures transferred from the polymer matrix and by the partially formed voids between the filler and matrix materials caused by insufficient interfacial bonding, which results in a weak structure (Shakuntala *et al.* 2014).

The flexural strength and elongation at break could be reduced by adding GO filler to a polymer matrix. This is due to the huge surface area and powerful van der Waals interactions and tendency towards agglomeration of GO particles (Eqra *et al.* 2021). These aggregates caused localized weak regions that lower the composite's overall flexural strength because they operate as stress concentrators inside the matrix. Filler aggregation in the matrix caused a raise in microscopic structural defects, which reduces performance. It is noteworthy to emphasize that flexural strength exceeded tensile strength. This is because, during the 3-point bend test, the entire volume of material experienced uniform stress (Hui et al., 2010; Manta *et al.* 2020).

The addition of filler impacted the bending load through the interaction between the filler particle and the resin, which was also responsible for the decreased flexural strength of the GO composites. This phenomena is frequently seen in polymer composites, where there is an ideal filler level that, when exceeded, causes the agglomeration effects to become more pronounced and result in a loss of characteristics (Nugraha *et al.* 2024).

3.7.3 Compression Analysis Results

The compression test results for pure resins and their GO composites are shown in Fig. 13(a). Fig.13(b) shows the stress-strain curve for pure resins and their GO composites. The curves display comparable patterns.

Table 7. Compression analysis results for pure resins and their 1 wt. % GO composites

Sample Code	Wt % of GO	Ultimate Force (N)	Ultimate Stress (MPa)	Total Elongation (%)
A1	0	4850	85.5	9.53
AG1	1	7120	75.9	5.56
B1	0	3290	87.7	8.07
BG1	1	7470	57.7	6.41
C1	0	3300	70.5	10.3
CG1	1	1990	18.6	5.60

The compressive strength and total elongation for GO composites decreased by 11.2% and 41.6%, respectively, based on the compressive study of the samples GP resin and its GO composites. The samples of ISO resin and its GO composites were analyzed compressively, and the results showed that the

compressive strength and total elongation of the GO composites reduced by 34.2 % and 20.5%, correspondingly. The overall elongation and compressive strength of the GO composites dropped by 73.6 % and 45.6%, respectively, according to the results of a compressive analysis carriedout on the RL resin samples and its GO composites.

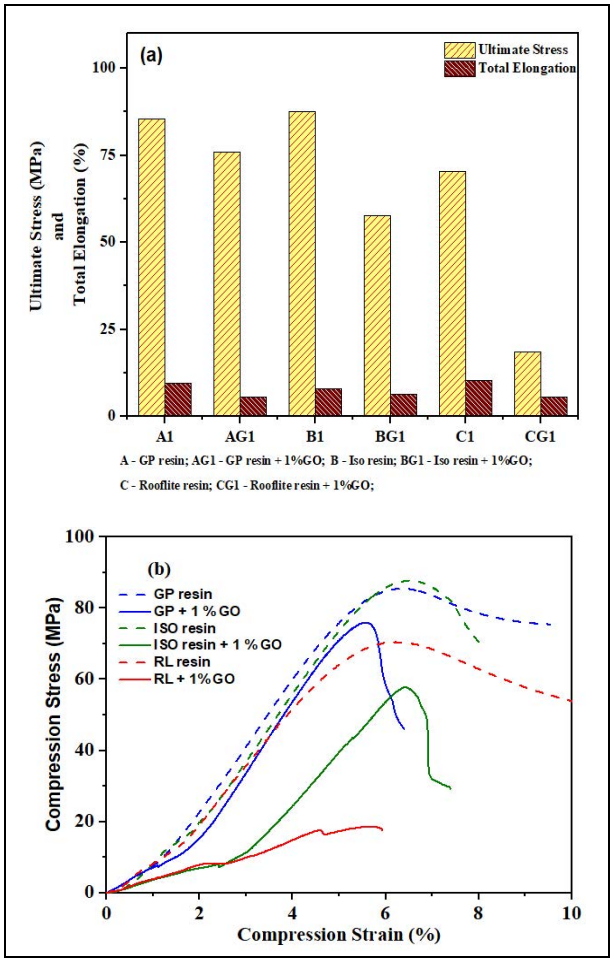


Fig. 13: (a) Compression analysis for pure resins and their 1 wt. % GO composites and (b) strain vs stress pure resins and their 1 wt. % GO composites

Pure resins had a greater ultimate strength in compression testing as a result of simultaneous void formation and increase in matrix porosity. The formation of voids might be due to inadequate dispersion of the GO filler within the resin matrix. The agglomeration caused by poorly dispersed nano fillers, such as GO, functions as stress concentrators and degrades the mechanical characteristics of composite materials (Li et al., 2013). According to Rafiee *et al.* (2010), the interfacial adhesion between the filler and the matrix plays a critical role in determining the mechanical performance of nanocomposites. Early failure and ineffective stress transfer are caused by poor bonding. Micro voids and other defects might develop in the composite structure as a result of unevenly distributed GO particles.

The highest compressive strength was found in GPR with 1% GO Composite, which was appropriate for more demanding structural applications where high compressive strength is crucial. Iso marine resin with 1% GO composite had a moderate compressive strength, making it suitable for maritime applications, where durability and strong compressive strength are vital. Due to its lower compressive strength, RL resin with 1% GO composite could be employed in structural applications that are less demanding or where cost and weight are more important considerations than high compressive strength.

3.8 Determination of Dielectric Strength

The results of dielectric strength study are presented in Table 8 and in Fig. 14.

Table 8. Breakdown voltage and dielectric strength for pure resins and their 1 wt. % GO composites

Sample Code	Weight % of GO	Breakdown voltage (V)	Dielectric Strength (V/mm)
A1	0	17,000	4076.73
AG1	1	15,100	5080.0
B1	0	18,000	3203.0
BG1	1	16,500	4615.4
C1	0	16,500	4342.1
CG1	1	15,500	4828.0

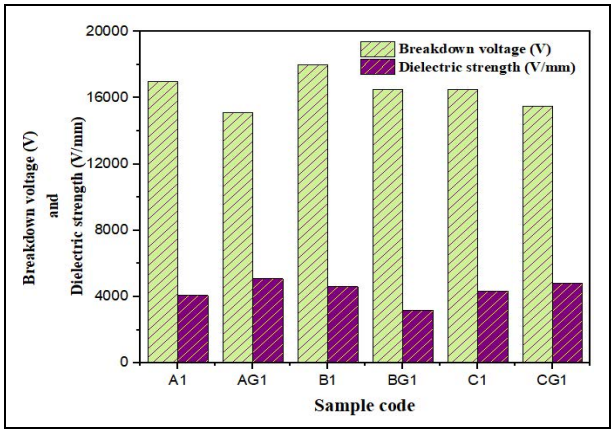


Fig. 14: Comparative analysis of dielectric strength of pure resins and their 1 wt. % GO composites

The dielectric strength of a material depends heavily on how well the filler is dispersed in the resin matrix and the strength of the interfacial bonds between them. Due to the good dispersion of GO in to the UPR matrix, the interaction between the polymer matrix and GO was strong, resulting in an enhanced overall dielectric performance by preventing electrical breakdown and improving the insulating properties of the material. Possibly another explanation is GO added to the

resin fills the micro voids and minimized the free volume in the composite, thereby reducing the possibility of charge accumulation and breakdown at high electric fields (Schneuwly *et al.* 1998). Moreover, the high surface area and layered structure of GO function as a barrier to the flow of charge carriers.

4. CONCLUSION

This study investigated the synthesis, characterization, and performance of UPR composites reinforced with 1 wt.% GO. The composites were prepared by mechanically mixing unsaturated polyester resins general-purpose resin, ISO resin and RL resin with GO, followed by ultrasonication and curing. The oxidation of graphene into GO and the generation of resin composites were verified by XRD and FTIR investigations. The SEM analysis showed improved particle distribution and morphological changes in the resin after GO incorporation. Thermogravimetric analysis and differential scanning calorimetry demonstrated the increased thermal stability, while the mechanical tests showed improvements in hardness. The dielectric strength of the composites also varied based on resin type, with GO improving insulation properties in certain resins. Overall, the addition of GO significantly enhanced the thermal, mechanical, and electrical properties of the polyester composites, making them suitable for advanced material applications.

ACKNOWLEDGMENTS

The authors would like to express their gratitude to the Principal and Head of the Chemistry Department at Government Arts College, Udumalpet, TN, India for the facilities provided to carry out the tests. Authors thank Dr. R. Venckatesh of the Chemistry Department of Government Arts College, Udumalpet, TN, India, for his assistance with the IR spectral analyses of the samples. The authors would like to express their gratitude to the department's DST FIST DST-FIST-2018 (SR/FST/COLLEGE-417/2018) (TPN-2011) laboratory for supporting this study.

AUTHOR CONTRIBUTIONS

M. Karunakaran and Ravi Subban – Conceptualization. A. Amutha and M. Karunakaran – Formal Analysis. M. Karunakaran, C. V. Vijayakumar and Ravi Subban – Supervision. A. Amutha and M. Karunakaran – Writing – original draft. M. Karunakaran, C. V. Vijayakumar and Ravi Subban – Writing – review & editing.

FUNDING

This research received no specific grant from any funding agency in the public, commercial, or not-for-profit sectors.

CONFLICTS OF INTEREST

The authors declare that there is no conflict of interest.

COPYRIGHT

This article is an open-access article distributed under the terms and conditions of the Creative Commons Attribution (CC BY) license (http://creativecommons.org/licenses/by/4.0/)



REFERENCES

Adeosun, S. O., Akpan E. I. and Akanegbu, H. A., Thermo-Mechanical Properties of Unsaturated Polyester Reinforced with Coconut and Snail Shells, *Int. J. Compos. Mater,* 5(3), 52-64(2015). https://doi.org/10.5923/j.cmaterials.20150503.02

Aghehrochaboki, R., Chaboki, Y. A., Maleknia, S.A. and Irani, V., Polyethyleneimine functionalized graphene oxide/methyldiethanolamine nanofluid: Preparation, characterization, and investigation of CO2 absorption, *J. Environ. Chem. Eng.,* 7(5), 103285(2019). https://doi.org/10.1016/j.jece.2019.103285

Ali, M., Khliwi, M. S., Kamel, F. and Jameel, R, Mechanical Properties Of new Composite Unsaturated Polyesters Based on Nano Fillers for Marine application, *J. Phys. Conf. Ser.,* 1294(5), 052075(2019). https://doi.org/10.1088/1742-6596/1294/5/052075

Alshammari, B. A., Mubaddel, F. S. A., Karim, M. R., Hossain, M., Mutairi, A. S. A. and Wilkinson, A. N., Addition of Graphite Filler to Enhance Electrical, Morphological, Thermal, and Mechanical Properties in Poly (Ethylene Terephthalate): Experimental Characterization and Material Modeling, *Polym.,* 11(9), 1411(2019). https://doi.org/10.3390/polym11091411

Ambika, M. R., Nagaiah, N., Harish, V., Lokanath, N. K., Sridhar, M. A., Renukappa, N. M. and Suman, S. K., Preparation and characterisation of Isophthalic-Bi2O3 polymer composite gamma radiation shields, *Radiat. Phys. Chem.,* 130, 351-358(2017). https://doi.org/10.1016/j.radphyschem.2016.09.022

An, J., Zhang, Y., Zhang, X., He, M., Zhou, Jiang, Zhou, Jin, Liu, Y., Chen, X., Hu, Y., Song, X., Chen, J., Wu, T., Kang, J. and Xie, Z., Structure and Properties of Epoxy Resin/Graphene Oxide Composites Prepared from Silicon Dioxide-Modified Graphene Oxide, *ACS. Omega.,* 9(15), 17577-17591(2024). https://doi.org/10.1021/acsomega.4c00707

Anegbe, B., Ifijen, I. H., Maliki, M., Uwidia, I. E. and Aigbodion, A. I., Graphene oxide synthesis and applications in emerging contaminant removal: a comprehensive review, *Environ. Sci. Eur.,* 36(1), 15(2024). https://doi.org/10.1186/s12302-023-00814-4

Arora, G. and Gupta, A., Mechanical and Structural Properties of Epoxy Resin-Allyl Guar Gum Composites, *Open Chem. Eng. J.,* 17(1), e187412312304120(2023). https://doi.org/10.2174/18741231-v17-e230505-2022-HT24-4379-1

Bastiurea, M., Bastiurea, M. S., Andrei, G., Murarescu, M. and Dumitru, D., Determination of Glass Transition Temperature for Polyester / Graphene Oxide and Polyester / Graphite Composite by TMA and DSC, *Ann "Dunarea Jos" Univ Galati Fascicle IX, Metall. Mater. Sci.,* 38(2), 32-36(2015).

Bastiurea, M., Rodeanu, M. S., Dima, D., Murarescu, M., Thermal and Mechanical Properties of Polyester Composites with Graphene Oxide and Graphite, *Dig. J. Nanomater. Biostruct.,* 10(2), 521-533(2015).

Bera, M., Chandravati, Gupta, P. and Maji, P. K., Facile One-Pot Synthesis of Graphene Oxide by Sonication Assisted Mechanochemical Approach and Its Surface Chemistry, *J. Nanosci. Nanotechnol.,* 18(2), 902-912(2018). https://doi.org/10.1166/jnn.2018.14306

Bing, N., Yang, J., Gao, H., Xie, H., Yu, W., Unsaturated polyester resin supported form-stable phase change materials with enhanced thermal conductivity for solar energy storage and conversion. Renew. Energy, 173, 926-933(2021). https://doi.org/10.1016/j.renene.2021.04.033

Bora, C., Gogoi, P., Baglari, S. and Dolui, S. K., Preparation of polyester resin/graphene oxide nanocomposite with improved mechanical strength, *J. Appl. Polym. Sci.,* 129(6), 3432-3438(2013). https://doi.org/10.1002/app.39068

Celebi, M., Karakas, K., Ertas, I. E., Kaya, M. and Zahmakiran, M., Palladium Nanoparticles Decorated Graphene Oxide: Active and Reusable Nanocatalyst for the Catalytic Reduction of Hexavalent Chromium (VI), *Chemistry Sel.,* 2(27), 8312-8319(2017). https://doi.org/10.1002/slct.201700967

Chen, Y., Qi, Y., Tai, Z., Yan, X., Zhu, F. and Xue, Q., Preparation, mechanical properties and biocompatibility of graphene oxide/ultrahigh molecular weight polyethylene composites, *Eur. Polym. J.,* 48(6), 1026-1033(2012). https://doi.org/10.1016/j.eurpolymj.2012.03.011

Dhali, S., Karakoti, M., Pandey, S., SanthiBhushan, B., Verma, R. K., Srivastava, A., Bal, R., Mehta, S. P. S., Sahoo, N. G., Graphene oxide supported Pd-Fe nanohybrid as an efficient electrocatalyst for proton exchange membrane fuel cells, *Int. J. Hydrogen. Energy.,* 45(37), 18704-18715(2020). https://doi.org/10.1016/j.ijhydene.2019.09.131

Dhanunjayarao, B., Sanivada, U. K., Naidu, N. S. and Fangueiro, R., Effect of graphite particulate on mechanical characterization of hybrid polymer composites, *J. Ind. Text.,* 51(2-suppl), 2594S-2615S(2022). https://doi.org/10.1177/15280837211010670

Edwards, E. R., Almeida, É. C., Santos, M. B. and Oliveira, A. S., Application of graphene oxide as (nano) reinforcement in epoxy composites, *Matéria.,* 27(2), e13177(2022). https://doi.org/10.1590/s1517-707620220002.1377

Eqra, R., Moghim, M. H. and Eqra, N., A study on the mechanical properties of graphene oxide/epoxy nanocomposites, *Polym. Polym. Compos.,* 29(9_suppl), S556-S564(2021). https://doi.org/10.1177/09673911211011150

Farshidfar, A., Bazgir, S., Katbab, A. A. and Vaziri, A., Manipulation of mechanical and thermal properties of graphene oxide/nanoclay/unsaturated polyester hybrid nanocomposites by the surface chemistry and nanofiller composition, *Polym. Test.,* 120, 107951(2023). https://doi.org/10.1016/j.polymertesting.2023.107951

Fryczkowski, R., Gorczowska, M., Ślusarczyk, C., Fryczkowska, B. and Janicki, J., The possibility of obtaining graphene/polymer composites from graphene oxide by a one step process, *Compos. Sci. Technol.,* 80, 87-92(2013). https://doi.org/10.1016/j.compscitech.2013.03.012

Goudarzi, R., Motlagh, G. H., Elhamnia, M. and Motahari, S., Graphite Nanosheet as Low Shrinkage Additive, Curing Accelerator, and Conducting Filler for Unsaturated Polyester Resin, *Polym. Plast. Technol. Eng.,* 55(12), 1231-1239(2016). https://doi.org/10.1080/03602559.2015.1132468

Goyal, R. K., Kambale, K. R., Nene, S. S., Selukar, B. S., Arbuj, S. and Mulik, U. P., Fabrication, thermal and electrical properties of polyphenylene sulphide/copper composites, *Mater. Chem. Phys.,* 128(1-2), 114-120(2011). https://doi.org/10.1016/j.matchemphys.2011.02.065

Hosseini, S. M., Soltanabadi, A., Abdouss, M. and Mazinani, S., Investigating the structure of the product of graphene oxide reaction with folic acid and chitosan: density functional theory calculations, *J. Biomol. Struct. Dyn.,* 40(24), 14146-14159(2022). https://doi.org/10.1080/07391102.2021.2001372

Hui, C., Hong, L., Li, Y., Jian-xin, L. and Li, Y., Study on the preparation and properties of novolac epoxy/graphite composite bipolar plate for PEMFC, *Int. J. Hydrogen. Energy.,* 35(7), 3105-3109(2010). https://doi.org/10.1016/j.ijhydene.2009.08.030

Idrisi, A. H. and Mourad, A. H. I., Fabrication and Wear Analysis of Aluminium Matrix Composite Reinforced by SiC Micro and Nano Particles, in: Volume 6A: Materials and Fabrication, *Am. Soc. Mech. Eng.,* 6, 16-20(2017). https://doi.org/10.1115/PVP2017-65459

Jdayil, B. A., Mourad, A. H. I. and Hussain, A., Investigation on the mechanical behavior of polyester-scrap tire composites, *Constr. Build. Mater.,* 127, 896-903(2016). https://doi.org/10.1016/j.conbuildmat.2016.09.138

Karunakaran, M., Subban, R., Thangamani, A. and Thangavel, V. C., Impact of Graphite on Unsaturated Polyester/graphite Composites for the Fabrication of Bipolar Plates, *Orient. J. Chem.,* 40(3), 815-828(2024). https://doi.org/10.13005/ojc/400325

Kim, H., Abdala, A. A., Macosko, C. W., Graphene/Polymer Nanocomposites, *Macromol.,* 43(16), 6515-6530(2010). https://doi.org/10.1021/ma100572e

Kumar, S. S. A., M., N. B., Batoo, K. M., Wonnie Ma, I. A., Ramesh, K., Ramesh, S. and Shah, M. A., Fabrication and characterization of graphene oxide-based polymer nanocomposite coatings, improved stability and hydrophobicity, *Sci. Rep.,* 13(1), 8946(2023). https://doi.org/10.1038/s41598-023-35154-z

Li, Z., Young, R. J., Wang, R., Yang, F., Hao, L., Jiao, W. and Liu, W., The role of functional groups on graphene oxide in epoxy nanocomposites, *Polym.,* 54(21), 5821-5829(2013). https://doi.org/10.1016/j.polymer.2013.08.026

Liu, P., Yao, Z. and Zhou, J., Mechanical, thermal and dielectric properties of graphene oxide/polyimide resin composite, *High. Perform. Polym.,* 28(9), 1033-1042(2016). https://doi.org/10.1177/0954008315613558

Liu, Q., Zhao, Y., Gao, S., Yang, X., Fan, R., Zhi, M. and Fu, M., Recent advances in the flame retardancy role of graphene and its derivatives in epoxy resin materials, *Compos. Part A. Appl. Sci. Manuf.,* 149, 106539(2021). https://doi.org/10.1016/j.compositesa.2021.106539

Manta, A., Gresil, M. and Soutis, C., Tensile and flexural behaviour of a graphene/epoxy composite: experiments and simulation, *J. Phys. Mater.,* 3(1), 014006(2020). https://doi.org/10.1088/2515-7639/ab52d8

Marcano, D. C., Kosynkin, D. V., Berlin, J. M., Sinitskii, A., Sun, Z., Slesarev, A., Alemany, L. B., Lu, W. and Tour, J. M., Improved Synthesis of Graphene Oxide, *ACS. Nano.,* 4(8), 4806-4814(2010). https://doi.org/10.1021/nn1006368

Misra, A., Tyagi, P. K., Singh, M. K., Misra, D. S., FTIR studies of nitrogen doped carbon nanotubes, *Diam. Relat. Mater.,* 15(2-3), 385-388(2006). https://doi.org/10.1016/j.diamond.2005.08.013

Mourad, A. H. I., Ayad, O. G., Rahman, A., Alnaqbi, A. H. and Jdayil, B. I. A., Experimental Investigation of Kevlar KM2Plus Nano-Reinforced Laminated Composite Thermo-Mechanical Properties, ASME 2016 Pressure Vessels and Piping Conference*, The American Society of Mechanical Engineers*, 1-7(2016). https://doi.org/10.1115/PVP2016-63857

Mourad, A. H. I., Jdayil, B. A., Hassan, M., Mechanical behavior of Emirati red shale fillers/unsaturated polyester composite, *SN. Appl. Sci.,* 2(3), 497(2020). https://doi.org/10.1007/s42452-020-2284-4

Nosal, H., Moser, K., Warzała, M., Holzer, A., Stańczyk, D., Sabura, E., Selected Fatty Acids Esters as Potential PHB-V Bioplasticizers: Effect on Mechanical Properties of the Polymer, *J. Polym. Environ.,* 29(1), 38-53(2021). https://doi.org/10.1007/s10924-020-01841-5

Nugraha, A. D., Kumar, V. V., Gautama, J. P., Wiranata, A., Mangunkusumo, K. G. H., Rasyid, M. I., Dzanzani, R., Muflikhun, M. A., Investigating the Characteristics of Nano-Graphite Composites Additively Manufactured Using Stereolithography, *Polym.,* 16(8), 1021(2024). https://doi.org/10.3390/polym16081021

Ossonon, B. D. and Bélanger, D., Synthesis and characterization of sulfophenyl-functionalized reduced graphene oxide sheets, *RSC. Adv.,* 7(44), 27224-27234(2017). https://doi.org/10.1039/C6RA28311J

Palomba, M., Longo, A., Carotenuto, G., Gel-Phase Reduction of Graphene Oxide Coatings by L-Ascorbic Acid, *Mater. Proc.,* 4(1), 33(2021). https://doi.org/10.3390/IOCN2020-07783

Patnaik, A., Satapathy, A., Mahapatra, S. S. and Dash, R. R., A Comparative Study on Different Ceramic Fillers Affecting Mechanical Properties of Glass—Polyester Composites, *J. Reinf. Plast. Compos.,* 28(11), 1305-1318(2009). https://doi.org/10.1177/0731684407086589

Rafiee, M. A., Rafiee, J., Srivastava, I., Wang, Z., Song, H., Yu, Z. and Koratkar, N., Fracture and Fatigue in Graphene Nanocomposites, *Small.,* 6(2), 179-183(2010). https://doi.org/10.1002/smll.200901480

Reis, T. M. C., Castro, V. G., Amurin, L. G. and Silva, G. G., Graphene oxide dispersion in epoxy resin prepared by direct phase transfer from ethanol: Rheology and aging, *Compos. Part C, Open Access.,* 10, 100340(2023). https://doi.org/10.1016/j.jcomc.2022.100340

Rochman, R. A., Wahyuningsih, S., Ramelan, A. H. and Hanif, Q. A., Preparation of nitrogen and sulphur Co-doped reduced graphene oxide (rGO-NS) using N and S heteroatom of thiourea, *IOP Conf. Ser. Mater. Sci. Eng.,* 509, 012119(2019). https://doi.org/10.1088/1757-899X/509/1/012119

Rusmirovic, J. D., Trifkovic, K. T., Bugarski, B., Pavlovic, V. B., Dzunuzovic, J., Tomic, M. and Marinkovic, A. D., High performances unsaturated polyester based nanocomposites: Effect of vinyl modified nanosilica on mechanical properties, *Express Polym. Lett.,* 10(2), 139-159(2016). https://doi.org/10.3144/expresspolymlett.2016.14

Salmah, H., Romisuhani, A. and Akmal, H., Properties of low-density polyethylene/palm kernel shell composites: Effect of polyethylene co-acrylic acid, *J. Thermoplast. Compos. Mater.,* 26(1), 3-15(2013). https://doi.org/10.1177/0892705711417028

Schneuwly, A., Groning, P., Schlapbach, L., Irrgang, C. and Vogt, J., Breakdown behavior of oil-impregnated polypropylene as dielectric in film capacitors, *IEEE Trans. Dielectr. Electr. Insul.,* 5(6), 862-868(1998). https://doi.org/10.1109/94.740768

Shakuntala, O., Raghavendra, G. and Kumar, A. S., Effect of Filler Loading on Mechanical and Tribological Properties of Wood Apple Shell Reinforced Epoxy Composite, *Adv. Mater. Sci. Eng.,* 2014, 1-9(2014). https://doi.org/10.1155/2014/538651

Sudesh, Kumar, N., Das, S., Bernhard, C. and Varma, G. D., Effect of graphene oxide doping on superconducting properties of bulk MgB 2, *Supercond. Sci. Technol.,* 26(9), 095008(2013). https://doi.org/10.1088/0953-2048/26/9/095008

Suherman, H., Dweiri, R., Sulong, A. B., Zakaria, M. Y. and Mahyoedin, Y., Improvement of the Electrical-Mechanical Performance of Epoxy/Graphite Composites Based on the Effects of Particle Size and Curing Conditions, *Polym.,* 14(3), 502(2022). https://doi.org/10.3390/polym14030502

Tang, J., Zhou, H., Liang, Y., Shi, X., Yang, X., Zhang, J., 2014. Properties of Graphene Oxide/Epoxy Resin Composites, *J. Nanomater.,* 2014(1), 696859(2014). https://doi.org/10.1155/2014/696859

Wang, H., Pei, X., Shao, R., Liu, S., Wang, W., Zhao, C. and Xu, Z., Resistance of Graphene/Epoxy Resin—Based Composite Materials to γ Radiation Damage and Their Mechanical Properties, *Coat.,* 13(9), 1536(2023). https://doi.org/10.3390/coatings13091536

Willis, M. R. and Masters, I., The effect of filler loading and process route on the three-point bend performance of waste based composites, *Compos. Struct.,* 62(3-4), 475-479(2003). https://doi.org/10.1016/j.compstruct.2003.09.021

Yang, X., Shang, S., Li, L., Layer-structured poly(vinyl alcohol)/graphene oxide nanocomposites with improved thermal and mechanical properties, *J. Appl. Polym. Sci.,* 120(3), 1355-1360(2011). https://doi.org/10.1002/app.33279

Zarei, V., Reinforcement of mechanical properties in unsaturated polyester resin with nanosheet, *Adv. Nano. Res.,* 16(1), 81-90(2024). https://doi.org/10.12989/anr.2024.16.1.081

Zhao, Z., Bai, P., Du, W., Liu, B., Pan, D., Das, R., Liu, C. and Guo, Z., An overview of graphene and its derivatives reinforced metal matrix composites: Preparation, properties and applications, Carbon N. Y, 170, 302-326(2020). https://doi.org/10.1016/j.carbon.2020.08.040